

Final Draft
of the original manuscript:

Hilgert, J.; Schmidt, H.N.B.; dos Santos, J.F.; Huber, N.:
Thermal Models for Bobbin Tool Friction Stir Welding
In: Journal of Materials Processing Technology (2010) Elsevier

DOI: 10.1016/j.jmatprotec.2010.09.006

Thermal Models for Bobbin Tool Friction Stir Welding

J Hilgert¹, H N B Schmidt², J F dos Santos¹, and N Huber¹

¹GKSS Forschungszentrum, Institute of Materials Research, Materials Mechanics,
Solid-State Joining Processes (WMP), Geesthacht, Germany

²HBS Engineering, Denmark

August 2, 2010

corresponding author: Jakob Hilgert, jakob.hilgert@gkss.de

Abstract

This study presents three thermal 3D models for bobbin tool Friction Stir Welding (FSW) implemented in Comsol and Matlab. The models use Thermal Pseudo Mechanical (TPM) heat sources and include tool rotation, an analytic shear layer model and ambient heat sinks like the machine and surrounding air. A new transient moving geometry approach has been implemented. It includes the full tool motion along the weld line, while the other two models use fixed geometry with and without moving heat source.

The computational effort is small for all three models. The steady state model can be solved in approximately 5 minutes on a state of the art workstation. Experiments on the FlexiStir experimental welding unit have been carried out to validate the models' outputs. The predictions of all models are in excellent agreement with each other and the experiment.

Keywords: Friction Stir Welding, FEM, Bobbin Tool

1 Introduction

Friction Stir Welding (FSW) is a solid state welding process developed and patented in 1991 at TWI by [Thomas et al., 1991]. It offers an alternative to conventional fusion welding processes providing a variety of excellent properties.

There is a class of FSW tools called bobbin tools (sometimes referred to as self reacting tools). The name refers to the shape of these tools, which consist of two shoulders connected by the tool pin. The tools can have a fixed gap or can allow force controlled welds by having an adjustable distance between the shoulders. When using a bobbin type tool there is no need for a backing plate as the loads act between the two shoulders and have to be carried only by the pin. This allows for welding machines with substantially lower stiffness but also yields a challenge in terms of tool design, material and lifetime. With bobbin tools it is possible to weld closed profiles, which makes the process very interesting for a wide range of applications. However, further development is needed to provide a robust bobbin tool process. As there is very little published in literature on this process the present work addresses the topic of thermal models for bobbin tool FSW.

Thermal modeling is a central part of FSW process simulation. This can be seen when reviewing the contributions on standard FSW: Many of the properties of a final weld can be derived directly from the thermal history of the work piece. Every process model in the field of FSW, be it micro-structural, CFD, or thermo-mechanical incorporates a thermal model or uses input data generated by one.

There are several possibilities to gain input parameters to any kind of FSW model.

[Zhang and Chen, 2008] use measured temperature data to construct a constant empirical thermal model for their numerical model.

When modeling FSW temperature fields, it can be important to know the power of the heat source (as used by [Lambrakos et al., 2003]). It has been proposed by [Vilaça et al., 2005] who presented a fully analytical model based on Rosenthal's equations and [Schmidt et al., 2004] to calibrate a model's power input variable (e.g. machine torque or heat source power) in order to minimize the difference between the model's predictions and experimental temperature measurements.

A related approach uses measurements of power such as machine power consumption or, more elaborately, torque at the tool to calculate the dissipated heat as done by [Khandkar et al., 2003], who calculate heat input from measured torque data assuming constant stress at the tool interface, or [Pew, 2006], who calculate heat input from an empirical torque model.

[Khandkar et al., 2006] distribute experimentally determined power to their numerical model in a quasi frictional way. Thereby the heat generation is proportional to the velocity of the tool interface.

The heat source can also be modeled using contact pressure p and Coulomb's friction coefficient μ as input parameters as proposed by [Frigaard et al., 2001] using a Coulomb friction model with variable coefficient to keep temperatures below the melting point. [Zhu and Chao, 2004] calibrate a Coulomb friction model with experimental data. Also [Schmidt and Hattel, 2005a] and [Mandal et al., 2008] use Coulomb friction with a constant coefficient as a heat source. [Zhang and Zhang, 2009] use Coulomb friction and additionally include slipping condition.

[Uyyuru and Kailas, 2006] use plastic dissipation in combination with Coulomb friction. This method has to deal with the difficulties of experimentally determining μ as a function of the temperature T and other factors.

[Colegrove and Shercliff, 2005] use viscous dissipation in their coupled CFD Model as an heat source. [Atharifar et al., 2009] additionally include Coulomb friction. The gap between purely thermal and coupled thermo-mechanical models was filled by [Schmidt and Hattel, 2008] who proposed the TPM model (see 2).

The most advanced Thermal model for bobbin tool FSW known to the authors was presented by [Deloison et al., 2008]. It uses a sequential 2D axisymmetric (flow) and 3D (thermal) coupling to calculate the steady state 3D heat source from results gained from an axisymmetric flow simulation. Transient results can be obtained when the heat source is tuned by experimentally determined time dependent torque values. Up to date the authors are not aware of a validated numerical model that can predict the 3D transient thermal field of a bobbin tool weld with no time dependent experimental input data needed. The models presented in this paper provide these capabilities in a fast and robust fashion with no need for inputs that are hard to determine experimentally such as the sticking coefficient δ or the friction coefficient μ . The Moving Geometry technique for Comsol that was implemented in the scope of the presented models is a new way of simulating moving tools without the need for any actual deformation calculated in the model. This makes the approach very fast as compared to fully coupled thermo mechanical Arbitrary Lagrangian Eulerian (ALE) models.

2 The Thermal Pseudo Mechanical (TPM) Heat Source

2.1 Contact Condition

The heat generation from the tool is governed by the contact condition between tool and base material. One can distinguish between sliding, sticking, or partial sliding and sticking. It is therefore convenient to define a contact state variable as proposed by [Schmidt et al., 2004] in (equation (1), equation (2), equation (3));

$$\delta = \frac{v_{matrix}}{v_{tool}} \quad (1)$$

$$\dot{\gamma} = v_{tool} - v_{matrix} \quad (2)$$

$$\delta = 1 - \frac{\dot{\gamma}}{v_{tool}} \quad (3)$$

where δ is the contact state variable, v_{matrix} the matrix velocity, v_{tool} the tool velocity and $\dot{\gamma}$ the shear rate. When assuming that the welding speed is small compared to the rotational velocities at the tool and matrix interface, which is true for most common welding parameter sets, one can derive the useful simplification equation (4)

$$\delta = \frac{\omega_{matrix}}{\omega_{tool}} \quad (4)$$

where ω_{matrix} is the matrix angular velocity and ω_{tool} the tool angular velocity. This contact state variable facilitates the formulation of analytical heat sources and is capable of representing any combination of sliding and sticking at the tool interface.

2.2 TPM Heat Source Equation

A promising new way of determining heat input without having to do an experimental calibration for every new set of welding parameters is the TPM approach proposed by [Schmidt and Hattel, 2008]. The method is based on the knowledge of the plastic behavior of the workpiece material at elevated temperatures. The yield stress is a function of temperature and dramatically decreases once it approaches the solidus temperature. This decrease is a natural limit to shear stresses present during welding. Shear stresses are of fundamental importance as they are the driving forces of heat generation. They are present in the terms for both frictional and plastic dissipative heating in the heat source equation equation (5).

$$q_{total} = \dot{\gamma}\tau_{friction} + (\omega_{tool}r - \dot{\gamma})\tau_{yield} \quad (5)$$

where q_{total} is the total heat flow, $\dot{\gamma}$ the shear rate, $\tau_{friction}$ the shear stress due to friction, τ_{yield} the shear yield stress, ω_{tool} the angular velocity of the tool and r the distance from the heat source center. Using the contact state variable equation (4) and Coulomb's law this can be expressed as equation (6).

$$q_{total} = \omega_{tool}r(\delta\tau_{yield} + (1 - \delta)\mu p) \quad (6)$$

where p is the uniform contact pressure and μ the Coulomb's friction coefficient. As long as the contact state is not pure sliding ($\delta \neq 0$), which can readily be assumed, it can be stated that the shear stress in the interface between tool and workpiece has to be equal to the yield shear stress equation (7).

$$\tau_{interface} = \tau_{friction} = \tau_{yield} \quad (7)$$

where $\tau_{friction}$ is the shear stress due to friction and $\tau_{interface}$ the shear stress at the interface between tool and workpiece. Inserting this into equation (6) results in the TPM heat source equation equation (8).

$$q_{total} = \omega_{tool}r\tau_{yield} \quad (8)$$

Now the only a priori unknown input parameter is the material property shear yield stress which is a function of mainly temperature and strain rate. Once this data is found experimentally, no further calibration is needed when changing other process parameters like welding speed, tool rotational speed or plate thickness. These parameters influence the solution as parameters in equation (6) (ω_{tool} , r) or as boundary conditions in the model.

3 Models

This work proposes three thermal FE models using a TPM heat source formulation. The abbreviation for the model types is as follows: Eulerian = eu, Lagrangian = lg and Moving Geometry = mg. The eu model uses a steady state Eulerian FE formulation. The lg and mg model the transient temperature field during a whole weld in a Lagrangian formulation. The lg model uses the standard Lagrangian approach. As a change of geometry objects during time dependent simulation is not supported by Comsol, there is no native way to have motion of a meshed tool along the weld line. On the contrary, it is very well possible to define time dependent expressions for the volume heat source term Q in the transient heat transfer equation (see equation (24) in sec. 3.2). The heat source is emulated by a set of time dependent regular expressions, which define a volume subset of the geometry to be the current heat source. This heat source volume is moved through the workpiece plane in the desired way with respect to time. The mg model, called the moving geometry model, uses step dependent remeshing and result mapping to enable the fully meshed tool to be moved along the weld line. All models are meshed with second order finite elements. Mesh size dependencies have been investigated to ensure that all the presented results represent a converged mesh.

Input Data

The implemented TPM heat sources rely on input data on temperature dependent shear yield stress. This can be derived from tensile yield stress data provided in the Metals Handbook of The American Society for Metals [197, 1979] by using the relationship from equation (9).

$$\tau_{yield} = \frac{\sigma_{yield}}{\sqrt{3}} \quad (9)$$

Where τ_{yield} is the shear yield stress and σ_{yield} the tensile yield stress. The resulting data is plotted in figure 1.

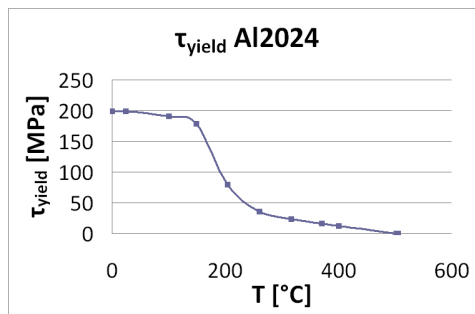


Figure 1: Calculated shear yield stress

As there is an inherent uncertainty regarding this data especially because the strain rate dependency is not included, the effect of errors in the shear-yield input data is investigated (see 5).

Analytical Shear Layer Model

All models in the present work can use an analytical shear layer model to prescribe heat flux in the workpiece to account for material moved around the pin in a shear layer. This model is based on previous work by [Schmidt and Hattel, 2005b] on standard FSW tool shear layers. It is designed to guarantee continuity at all boundaries, that is the pin and both shoulders, while it allows for a large amount of freedom in calibration. The model consists of six equations. equation (11) and equation (12) deal with the distance to the tool shoulders, equation (13) controls the designed

boundary shape of the shear layer, (equation (10), equation (14)) deal with the distance from the tool pin, and equation (15) defines the velocity field.

$$dr = r - R_p \quad (10)$$

$$dz = \frac{t_{plate}}{2} - |z| \quad (11)$$

$$\zeta = \frac{2dz}{t_{plate}} \quad (12)$$

$$R_* = (1 - \zeta^{m_{shape}}) \cdot R_s + \zeta^{m_{shape}} \cdot R_m \quad (13)$$

$$\rho = \frac{dr}{R_* - R_p} \quad (14)$$

$$v_{sl} = \omega r \cdot \sqrt{(1 - (\zeta^{m_z} \cdot \rho^{m_r}))^2} \quad (15)$$

Here dr is the normal distance from tool pin surface, R_p the tool pin radius, d_z the normal distance from nearest tool shoulder surface, t_{plate} the plate thickness, z the Z-coordinate, ζ the normalized d_z , R_* the shear layer outer boundary radius, m_{shape} the shear layer shape control variable, R_s the tool shoulder radius, R_m the shear layer minimum outer radius, ρ the normalized dr , v_{sl} the shear layer tangential velocity, m_z the shear layer shape control variable for z direction, and m_r the shear layer shape control variable for r direction (See figure 2).

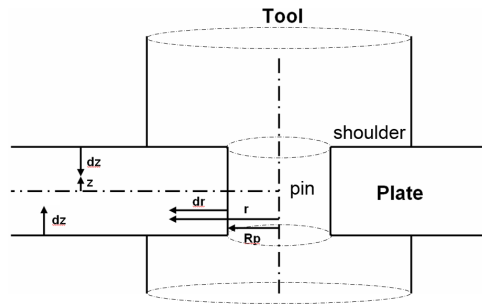


Figure 2: Shear layer coordinate system

The resulting v_{sl} tangential velocity field can then be split up into x and y components and added to the velocity u term in equation (16). It is mandatory to define a cutoff distance in r direction for the shear layer, which should be equal or near the shoulder radius. This can be done using regular expressions or by defining a suited sub domain. Else the continuity guaranteed by the formulation will extend the shear layer to a virtual infinitely large rotation shoulder, which is of course not desired.

The model uses fitting variables m_z , m_r , m_{shape} and R_m to provide flexible control over the the horizontal and vertical shearing velocities characteristics as well as shape of the boundary between shear layer and non sheared base material.

3.1 Eulerian Thermal Model

The Eulerian model includes a section of the workpiece, the clamps and the bobbin tool. The model boundaries are subject to boundary conditions corresponding to the actual welding process. Using the velocity term u in the steady state heat transfer equation equation (16), a convective heat flow is prescribed in the entire workpiece and the clamps corresponding to the welding speed.

$$\nabla(-k\nabla T) = Q - \rho c_p \mathbf{u} \nabla T \quad (16)$$

where k is the thermal conductivity, T the temperature, Q the total heat input, ρ the density, c_p the specific heat and \mathbf{u} the convection term in the heat transfer equation. The volumetric heat source term Q is zero in the Eulerian model. The heat input is prescribed as a surface flux of q_{total} (see equation (8)) at the interface between the tool and the workpiece. The tool rotation is represented by a convective flow. Different rotational orientations can be prescribed for the upper and lower shoulder. In the same way the shear layer is represented using the analytical shear layer model. All velocity terms are superposed to generate the Comsol convective flux term variable. The outlet surface at the trailing side is set to have only heat flux associated with the material moving at welding speed (see equation (17)).

$$-\mathbf{n} \cdot (-k\nabla T) = 0 \quad (17)$$

The inlet surface at the leading side (the not yet welded side) is set to have constant temperature. The workpiece and clamp surface as well as the tool surfaces, except for the upper one connected to the machine spindle, are set to have a constant heat transfer coefficient $h = h_{air} = 10 [W/m^2K]$. Thus heat is transferred to the surrounding air at room temperature $T_{inf} = (273.15 + 20)K$ according to equation (18).

$$-\mathbf{n}(-k\nabla T + \rho c_p \mathbf{u}T) = q_0 + h(T_{inf} - T) \quad (18)$$

Where \mathbf{n} is the surface normal vector, h the heat transfer coefficient, q_0 the prescribed inward surface heat flux and T_{inf} the external temperature. In the same way heat transfer is realized at the interface between tool and machine using $h = h_{spindle} = 500 [W/m^2K]$.

Steady State

The first approach to model the thermal field of the bobbin tool FSW process is to compute a steady state solution from an Eulerian model.

The amount of mesh elements needed for the tool and its close surroundings is very large compared to the amount needed for the remote parts of the specimen and clamping. Therefore it does not greatly influence the overall computational cost to include the total setup in the model as well. This way it is much easier to define meaningful boundary conditions and it also facilitates the comparison between the different model types.

3.2 Lagrangian Thermal Model

Modified TPM Heat Source

In the Lagrangian model the material is attached to the mesh. Therefore the movement of the plates relative to the tool is not represented by a convective heat flux as in the Eulerian model, but by a translation of the heat source as a function of time. Tool itself cannot be included in the standard Lagrangian formulation in Comsol. Therefore heat input has to be modified. In the Eulerian model it was defined as a surface flux at the interface between the tool and the workpiece. In the Lagrangian model this is replaced by a volume heat source at a time dependent location. The shape of this heat source volume is designed to be a close representation of the interface between the (virtual) tool and the workpiece. It is controlled by global regular expressions (equation (19), equation (20), equation (21), equation (22), equation (23)),

$$q_{surface} = \omega_{tool} \tau(T) r \quad (19)$$

$$q_{volume} = (hs_{us} + hs_p + hs_{ls}) \frac{q_{surface}}{t_{hl}} \quad (20)$$

$$hs_{us} = r > R_p \vee r < R_s \vee z > \left(\frac{t_{plate}}{2} - t_{hl}\right) \vee z < \frac{t_{plate}}{2} \quad (21)$$

$$hs_{ls} = r > R_p \vee r < R_s \vee z < \left(-\frac{t_{plate}}{2} + t_{hl}\right) \vee z > -\frac{t_{plate}}{2} \quad (22)$$

$$hs_p = r > R_p \vee r < (R_p + t_{hl}) \vee z > -\frac{t_{plate}}{2} \vee z < \frac{t_{plate}}{2} \quad (23)$$

where $q_{surface}$ is the TPM surface heat source, q_{volume} the volume heat source, z the Z-coordinate, t_{hl} the heat source layer thickness, hs_{us} a logical expression with $hs_{us}=1$ if (x,y,z) is in upper shoulder HS volume, hs_p a logical expression with $hs_p=1$ if (x,y,z) is in pin HS volume, and hs_{ls} a logical expression with $hs_{ls}=1$ if (x,y,z) is in lower shoulder HS volume,

The volumetric heat source term Q in the transient heat transfer equation equation (24) is prescribed to be q_{volume} given in equation (20). Therefore all the heat is generated in a finite volume around the tool.

$$\rho c_p \frac{\partial T}{\partial t} + \nabla(-k \nabla T) = Q - \rho c_p \mathbf{u} \nabla T \quad (24)$$

Boundary Conditions

The boundary conditions applied to the Lagrangian model are equal to those described for the Eulerian model in sec. 3.1 except for three differences:

- there is no constant convective flux in the workpiece and the clamps, as the heat source is moved and not the workpiece.
- there is a different heat source formulation (as described above).
- there is no tool, therefore the heat flux to the machine is located directly on the workpiece.

Transient Behavior

As the Lagrangian model captures the transient temperature field during the entire weld, the main advantage of the Lagrangian formulation over the Eulerian one is the capability of including a realistic preheating as the tool slowly enters the workpiece. Another advantage is the full thermal history of the cooling phase, which can be of great interest for metallurgical reactions (i.e. phase transformations, precipitate coarsening etc.) and residual stress investigations. A main drawback of this model is the missing tool. The emulation using boundary conditions like prescribed heat flux cannot fully reproduce the rotating tool. Therefore the moving geometry model has been implemented.

3.3 Moving Geometry Model

Motivation

As the pure Lagrangian model is limited to static mesh and therefore static geometry, it is impossible to include the tool. The memory and computational cost is also a limiting factor, as the whole weld length has to be meshed sufficiently fine to deal with the large gradients that occur in the close vicinity of the tool:

- temperature gradients

- convective flux gradients from tool rotation
- heat source gradients defined by regular expressions

All these limitations can be overcome by using an Arbitrary Lagrangian Eulerian (ALE) style approach. The shear layer, tool rotation and heat source are treated as in the Eulerian model while the relative translation between tool and work pieces is achieved by regenerating the geometry of the tool at the correct time dependent position for a number of discrete time steps (for details see section Modeling and Scripting). The mesh is regenerated with respect to the new geometry and the temperature field is transferred from the last time step using interpolation. The mesh is only refined in the vicinity of the tool and is coarse in the more remote regions of the model, thus saving memory and computational cost as compared to the Lagrangian model. A similar approach has been demonstrated by [Carbone et al., 2007] for a local flow model moving within a global thermal model. Although that model does not contain any elements that are moved through the void surroundings (air), as is the bobbin tool, it can still be adapted and applied to the present circumstances by using a new strategy of intermediate mapping.

Modeling and Scripting

The movement and mapping behavior is implemented using Matlab scripting. Comsol offers predefined functions for mesh generation and mapping but they were not designed for a moving geometry model. Therefore there are some serious challenges in developing a consistent model. As the tool is moving through empty space, temperature field mapping of the last time step results yields problems on the leading and trailing side (in front and behind the tool). The leading side is moved into a region where there was void space with no temperature information in the last time step, but which is the source for the temperature field mapping. Thus the elements at the leading side are assigned a temperature of 0K by the default Comsol interpolation algorithm if they are moved into the void by more than the extrapolation tolerance of the Comsol mapping algorithm. This would correspond to a very large effective heat flux out of the leading side of the tool, which is of course not correct (see figure 3).

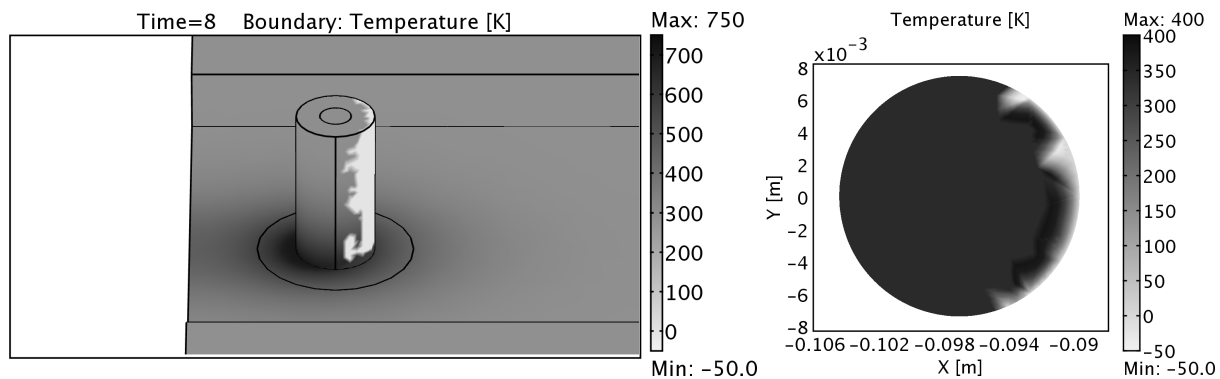


Figure 3: Insufficient mapping at the leading side

In the same way there would be a effective convective heat flux out of the tool on the trailing side, as parts of the tools thermal field of the last step get mapped to void and thereby disappear. These problems must be solved in order to be able to use the moving geometry approach. The solution used in the present work includes an intermediate mapping step between any two time steps. The latest results are mapped to a model of the tool and a model of the static geometry independently. The model of the tool is then translated to the new position for the next time step by changing the mesh coordinates. Then the model for the new time step is generated and the initial values are taken from the two partial intermediate models. The temperature values

from the partial model representing the tool are used at location where there is temperature information from both partial models available. In this way the mapping can be done without losses due to the nonphysical heat fluxes described above. Additionally the default Comsol interpolation and mapping algorithms are replaced by customized Matlab code. It controls the interpolation and extrapolation behavior while mapping such that any NaN or 0K mapping values that may result from varying element shape and size in time are replaced by applying a next neighbor extrapolation. This is necessary because the default mapping algorithm extrapolates values only within the distance of a certain ratio of an element size and results in NaN if the requested coordinate is further away from the available source. Because of the remeshing the curved surfaces of the tool are represented by different polygons for each time step. Therefore the requested mapping targets can sometimes be outside the mapping source geometry. The discrete time steps are chosen with respect to the welding speed to guarantee that the discrete steps in tool position are no larger than a chosen fraction of the tool diameter. The moving geometry algorithm can be abstracted as follows:

Algorithm 1 Moving Geometry Algorithm

```

generate model.geometry
mesh model
generate toolmodel.geometry
mesh toolmodel
generate staticmodel.geometry
mesh staticmodel
for all timesteps do
    solve timestep
    store solution
    map model → toolmodel
    map model → platemodel
    translate toolmodel.mesh
    update model.geometry
    mesh model
    map model ← toolmodel
    map model ← platemodel
end for

```

Boundary Conditions

The boundary conditions applied to the moving mesh model are the same as those described for the Eulerian model in (sec. 3.1), except for the convective flux through the workpiece and the clamps. This is not needed as the tool is moved and not the workpiece.

4 Experiments

The validation of the models has been done using experimental results from the FlexiStir advanced experimental device. Aluminum 2024 sheets in T3 condition with a thickness of 4mm have been welded using a bobbin tool with 13mm scrolled shoulders and a 5mm threaded pin with three flats. The plates welded were [250mm x 150mm] each. A starting notch was machined to facilitate the run-in. A parameter study has been carried out in advance in order to establish optimal process conditions with regards to the welding machine and weld quality. The welds used for the validation of the models were performed at 1100RPM with a welding speed of 21 [mm/min]. Three welds were produced with identical parameters to allow statistical evaluation. The temperatures were recorded using 18 type-k thermocouples located in the distances of 10,

15 and 20 [mm] from the weld line on the advancing and retreating side in the beginning, middle and end of the weld.

5 Results and Discussion

Characteristic Values

The thermal field results of all models have been compared. Therefore it is beneficial to define characteristic values that allow fast comparison not only between different models but also to experimental data. This study concentrates on two basic ones, which are illustrated in figure 4

T_{max} the maximum temperature at a certain location during the whole weld. This location is often addressed using side and distance data e.g. $T_{max_{as10}}$ for the maximum temperature on the advancing side 10mm from the weld line. It has to be stated that this scheme lacks information like X- and Z-position of the measurement. These can be of great influence especially in a Lagrangian model. Therefore it should always be considered to give fully qualified position information with a T_{max} value.

ΔP_T the peak width of the temperature profile $T(t)$ at a given location. The width is measured as the time over a given temperature T . The same aspects as stated above concerning location information also apply to the ΔP_T peak width. An example of a complete statement could look like this: The peak width ΔP_{400K} 10mm from the weld line on the advancing side at mid thickness of the plate at the half of the weld length is 12s.

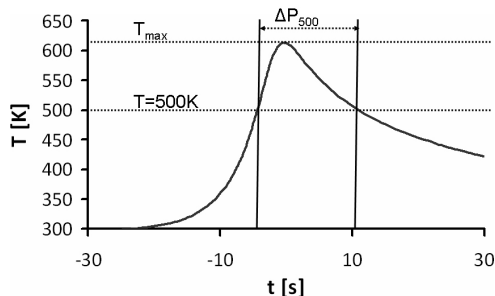


Figure 4: Characteristic values for result comparison

Shear Yield Data

The effect of errors in the shear yield input data is investigated by comparing results generated by identical models using three different shear yield functions. The original data (see 3) and two datasets scaled by +10% and -10% have been used. The temperature profiles predicted at as10 are compared in figure 5.

The model results show a weak dependency on the τ_{yield} input data. The temperature differences do not exceed 5K in the tested setups with variations in the τ_{yield} input data of $\pm 10\%$. Therefore the TPM models can be considered very robust when it comes to material data uncertainties.

Preheating

As bobbin tools are loaded significantly higher than single sided shoulder and pin tools it is of great importance to include a dwelling step at the beginning of the welding process. This is done to soften the material before the actual welding forces act on the pin. Usually the tool is positioned in a way that the pin is located in a notch or bore hole in the workpiece so that only

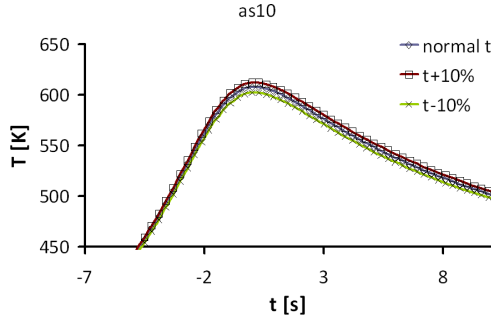


Figure 5: Temperature Differences Resulting from τ_{yield} Variations

the rotating shoulders are in tight contact. After sufficient preheating is achieved the translation of the tool is started thus forming the weld. The effect of including a dwelling and preheating step in the model is shown in figure 6.

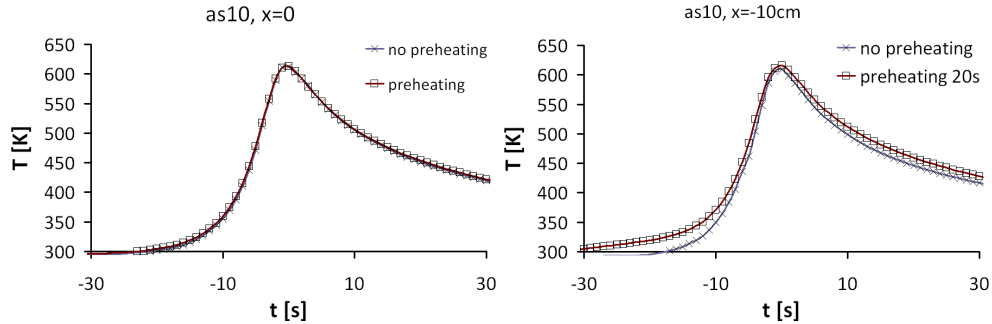


Figure 6: Effect of Preheating - Left: Thermocouples positioned in the middle of the weld line length Right: Thermocouples positioned 10cm towards the beginning of the weld - 2.5cm from the edge of the plate

Two cases are investigated by shifting the thermocouple position from the center of the weld line 100mm towards the start of the weld line. It can be seen that the effect of preheating is a rather local one. As expected the peak temperature as well as the temperature peak width are slightly increased at the position 25mm from the edge of the plate at the beginning of the weld. After 100mm of welding the effect has decayed and is no longer significant. It can be concluded that a preheating step has an influence on the very beginning of the weld. This influence can be predicted with the transient models and taken into account for short welds. For longer welds the influence of a preheating step is not of great importance, as the steady state of the welding process is not significantly affected even by relatively intense preheating.

Comparing Model Types

The three models are compared regarding their temperature field outputs. To preserve comparability, the chosen parameters do not include preheating, as it is not supported in the Eulerian model. The results are given as temperature profile plot in figure 7.

It can be stated that the models' predictions are in very good agreement.

The selection of the model type has fundamental consequences. It defines the computational effort and the model's capability to predict transient phenomena especially at the beginning of the weld. The results prove that the fast Eulerian model can be used as long as the area of interest is not within the region in which extensive influence of the preheating occurs when the tool slowly enters the workpiece. The differences in the prediction of peak temperature and peak

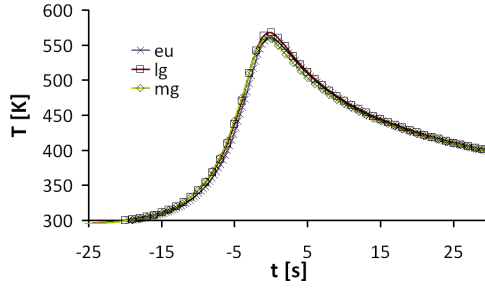


Figure 7: Model Results Comparison at as10

Table 1: Statistic Evaluation

	ΔT_{max}	ΔP_{400K}
absolute mean	3.5K	6.2s
relative mean	0.6%	3.3%
absolute standard deviation	6.2K	5.2s
relative standard deviation	1.1%	2.9%

width are very small. The mean standard deviation of the respective temperature values is only 1.6K, and the mean standard deviation of the respective peak width values is below 1s. Using the Eulerian model will save computational time with a factor in the range of 70 to 100 compared to the full moving geometry model.

In cases where a full and accurate thermal history of the entire weld line must be obtained, a combination of one of the transient model types and the Eulerian model can be chosen. This way only the beginning and the end of the weld have to be modeled transiently, thus greatly reducing the overall solution time.

Model Predictions

The temperature predictions for a weld in 4mm thick Al2024 with a 5mm pin and 13mm shoulder bobbin tool are given in figure 8. The welding speed is $800 \frac{mm}{min}$ at 400RPM. The position of the plotted data is in mid thickness of the plate. The predicted heat source power ranges from 1.42kW after preheating to 1.47kW at the end of the weld.

Experimental Validation

Table 1 compares peak temperatures and peak width differences between experimental (see sec. 4) and numerical data. Three experiments with identical parameters are considered giving a total of 18 temperature and 18 peak width variables to be compared with the model predictions. The table shows the mean temperature differences [K] and the mean peak width differences [s]. It also includes the standard deviation of the samples. All data is given as absolute value and relative to the numerical predictions.

The observed error in peak temperature is within the limit of accuracy of the temperature measurements. A typical example for the differences between experimental and model temperature data is given in figure 9. It can be seen that the cooling rate in lower temperature regions is over predicted by the model. This is believed to be due to the fact that only a finite part of the welding machine, which acts as heat sink, is included in the model. This effect will be further investigated in future work.

Conclusions

Three thermal numerical 3D models for bobbin tool FSW are proposed. The Eulerian model

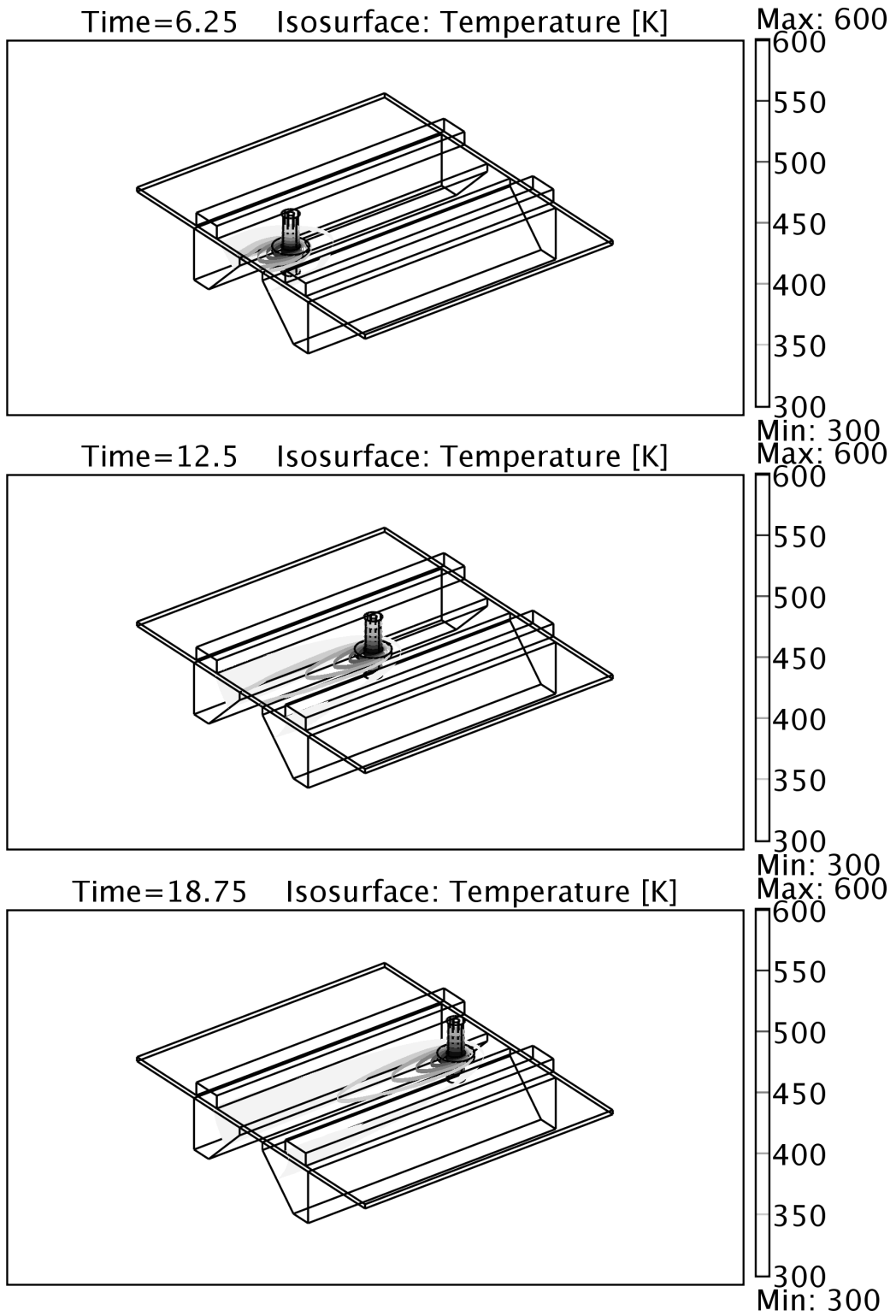


Figure 8: Temperatures predictions at the beginning, middle and end of the weld

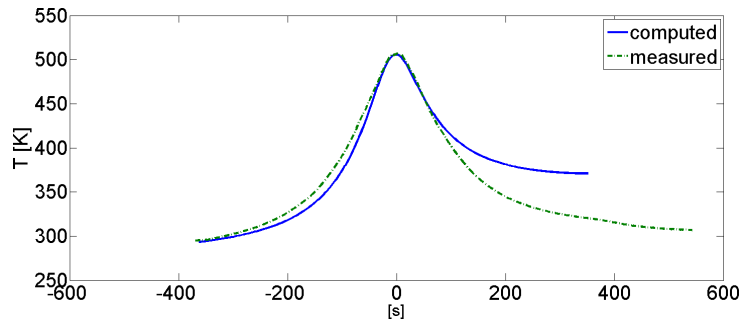


Figure 9: Temperatures differences between experimental and model data

predicts a steady state. The Lagrangian model is suited for short welds and predicts a transient temperature field. It cannot include the tool and the size of the workpiece is limited by the available computational resources as the whole weld line needs to have a fine mesh. The new moving geometry modeling approach can provide transient temperature histories of the tool and workpieces. It can be used for long welds as the mesh needs to be refined only in the vicinity of the tool. It can capture the effect of the heating up of the tool. The predictions of all three models can be compared for a steady state situation and agree very well.

Experimental validation has been conducted and shows that the mean deviation of the model's prediction of the peak temperature is only 3.5K. The peak width is predicted with a mean deviation of only 3.3%. It can therefore be concluded that the model's output can be used as an input for further work that depends on these values. An example for this could be microstructure or residual stress models. The deviations in final cooldown behaviour need further consideration, though. The influence of a preheating phase can be predicted with the transient models and taken into account for short welds. For longer welds the influence of this is small, as the steady state of the welding process is not significantly affected even by relatively intense preheating. The results prove that a TPM heat source in combination with a shear layer model is a valid heat source representing the FSW process using a bobbin tool.

Acknowledgements

This work was carried out at and kindly supported by GKSS Forschungszentrum GmbH, Institute of Materials Research, Materials Mechanics and Joining, Solid-State Joining Processes (WMP), Geesthacht, Germany and DTU, Copenhagen, Denmark.

References

- [197, 1979] (1979). *Metals Handbook*, page 75. The American Society for Metals, 9th edition.
- [Atharifar et al., 2009] Atharifar, H., Lin, D., and Kovacevic, R. (2009). Numerical and experimental investigations on the loads carried by the tool during friction stir welding. *Journal of Materials Engineering and Performance*, 18(4):339–350.
- [Carbone et al., 2007] Carbone, R., Langella, A., and Nele, L. (2007). Numerical modelling of a time - dependent friction stir welding process with a moving tool using comsol script. In *COMSOL Users Conference 2007 Grenoble*. Dipartimento di Ingegneria dei Materiali e della Produzione - DIMP.
- [Colegrove and Shercliff, 2005] Colegrove, P. and Shercliff, H. (2005). 3-dimensional cfd modelling of flow round a threaded friction stir welding tool profile. *Journal of Materials Processing Technology*, 169:320–327.

- [Deloison et al., 2008] Deloison, D., Jacquin, D., Gurin, B., Desrayaud, C., and Marie, F. (2008). Simplified models for bobbin-tool fsw process. In dos Santos, J. F., editor, *3rd FSW Modelling and Material Flow Visualisation Seminar*, Geesthacht.
- [Frigaard et al., 2001] Frigaard, O., Grong, O., and Midling, O. (2001). A process model for friction stir welding of age hardening aluminum alloys. *Metallurgical and materials transactions A*, 32(A):1189–1200.
- [Khandkar et al., 2003] Khandkar, M., Khan, J., and Reynolds, A. (2003). Prediction of temperature distribution and thermal history during friction stir welding: input torque based model. *Science and Technology of Welding and Joining*, 8(3):165–174.
- [Khandkar et al., 2006] Khandkar, M., Khan, J., Reynolds, A., and Sutton, M. (2006). Predicting residual thermal stresses in friction stir welded metals. *Journal of Materials Processing Technology*, 174(1-3):195–203.
- [Lambrakos et al., 2003] Lambrakos, S., Fonda, R., Milewski, J., and Mitchell, J. (2003). Analysis of friction stir welds using thermocouple measurements. *Science and Technology of Welding & Joining*, 8:385–390.
- [Mandal et al., 2008] Mandal, S., Rice, J., and Elmustafa, A. (2008). Experimental and numerical investigation of the plunge stage in friction stir welding. *Journal of Materials Processing Technology*, 203:411–419.
- [Pew, 2006] Pew, J. (2006). A torque-based weld power model for friction stir welding. Master’s thesis, Brigham Young University.
- [Schmidt and Hattel, 2005a] Schmidt, H. and Hattel, J. (2005a). A local model for the thermo-mechanical conditions in friction stir welding. *Modelling Simul. Mater. Sci. Eng.*, 13:77–93.
- [Schmidt and Hattel, 2005b] Schmidt, H. and Hattel, J. (2005b). Modelling heat flow around tool probe in friction stir welding. *Science and Technology of Welding and Joining*, 10(2):167–186.
- [Schmidt and Hattel, 2008] Schmidt, H. and Hattel, J. (2008). Thermal modelling of friction stir welding. *Scripta Materialia*, 58(5):332–337.
- [Schmidt et al., 2004] Schmidt, H., Hattel, J., and Wert, J. (2004). An analytical model for the heat generation in friction stir welding. *Modelling and Simulation in Materials Science and Engineering*, 12(1):143–157.
- [Thomas et al., 1991] Thomas, W., Nicholas, E., Needham, J., Murch, M., Templesmith, P., and Dawes, C. (1991). Friction stir welding.
- [Uyyuru and Kailas, 2006] Uyyuru, R. and Kailas, S. (2006). Numerical analysis of friction stir welding process. *Journal of Materials Engineering and Performance*, 15(5):505–518.
- [Vilaça et al., 2005] Vilaça, P., Quintino, L., and dos Santos, J. (2005). IStir - analytical thermal model for friction stir welding. *Journal of Materials Processing Technology*, 169(3):452–465.
- [Zhang and Chen, 2008] Zhang, Z. and Chen, J. (2008). The simulation of material behaviors in friction stir welding process by using rate-dependent constitutive model. *J Mater Sci*, 43:222–232.
- [Zhang and Zhang, 2009] Zhang, Z. and Zhang, H. (2009). Numerical studies on controlling of process parameters in friction stir welding. *Journal of Materials Processing Technology*, 209(1):241–270.

[Zhu and Chao, 2004] Zhu, X. and Chao, Y. (2004). Numerical simulation of transient temperature and residual stresses in friction stir welding of 304l stainless steel. *Journal of Materials Processing Technology*, 146(2):263–272.